Environmental Research 263 (2024) 120085

Contents lists available at ScienceDirect

Environmental Research

journal homepage: www.elsevier.com/locate/envres

EDDS application destabilizes soil organic matter in phytoremediation: Insights from quantity and molecular composition of dissolved organic matter

Yan-ping Zhao [a], Peng-ran Guo [a,*], Zhi-liang Chen [b,**], Jin-li Cui [c], Jian-xu Wang [d], Chao Chen [a], Hang Wei [b], Cheng Wang [e]

[a] Guangdong Provincial Key Laboratory of Chemical Measurement and Emergency Test Technology, Guangdong Provincial Engineering Research Center for Online Monitoring of Water Pollution, Institute of Analysis, Guangdong Academy of Sciences (China National Analytical Center, Guangzhou), Guangzhou, 510006, China
[b] South China Institute of Environmental Sciences, Ministry of Eology and Environment, Guangzhou, 510006, China
[c] Key Laboratory for Water Quality and Conservation of the Pearl River Delta, Ministry of Education, School of Environmental Science and Engineering, Guangzhou University, Guangzhou, 510006, China
[d] State Key Laboratory of Environmental Geochemistry, Institute of Geochemistry, Chinese Academy of Sciences, Guiyang, 550082, China
[e] Jiangsu Key Laboratory of Atmospheric Environment Monitoring and Pollution Control, Collaborative Innovation Center of Atmospheric Environment and Equipment Technology, School of Environmental Science and Engineering, Nanjing University of Information Science and Technology, Nanjing, 210044, China

ARTICLE INFO

Keywords:
Soil organic matter
Dissolved organic matter
Priming effect
Carbon emission
Chelating agent
Fourier-transform ion cyclotron resonance mass spectrometry

ABSTRACT

The stability of soil organic matter (SOM) is crucial for metal transport and carbon cycling. S,S-ethylenediaminedisuccinic acid (EDDS) is widely used to enhance phytoremediation efficiency for heavy metals in contaminated soils, yet its specific impacts on SOM have been underexplored. This study investigates the effects of EDDS on SOM stability using a rhizobox experiment with ryegrass. Changes in soil dissolved organic matter (DOM) quantity and molecular composition were analyzed via Fourier transform ion cyclotron resonance mass spectrometry. Results showed that the use of EDDS increased the uptake of Cu, Cd and Pb by ryegrass, but simultaneously induced the destabilization and transformation of SOM. After 7 days of EDDS application, dissolved organic carbon (DOC) and nitrogen (DON) concentrations in rhizosphere soils increased significantly by 3.44 and 10.2 times, respectively. In addition, EDDS reduced lipids (56.3%) and proteins/amino sugars-like compounds (52.1%), while increasing tannins (9.11%) and condensed aromatics-like compounds (24.4%) in the rhizosphere DOM. These effects likely stem from EDDS's dual action: extracting Fe/Al from SOM-mineral aggregates, releasing SOM into the DOM pool, and promoting microbial degradation of bioavailable carbon through chain scission and dehydration. Our study firstly revealed that the application of EDDS in phytoremediation increased the mineralization of SOM and release of CO_2 from soil to the atmosphere, which is important to assess the carbon budget of phytoremediation and develop climate-smart strategy in future.

1. Introduction

Soil organic matter (SOM) constitutes the largest carbon pool in terrestrial ecosystem (Beillouin et al., 2023). Recently, the stability of SOM has received great attention, because a small change in the turnover of soil C can influence the emission of CO_2 to atmosphere and affect global C cycling (Chen et al., 2019). Heavy metal pollution is a global issue in soils, with particularly high proportions (13.3%) of soil contamination occurring in China (Zhao et al., 2015; Antoniadis et al., 2019; Wang et al., 2023). Chelate-assisted phytoremediation is one of the most widely used technologies for remediating soils contaminated by heavy metals (Garbisu and Alkorta, 2001; Harmon, 2022). S, S-ethylenediaminedisuccinic acid (EDDS), a biodegradable chelating agent, is frequently applied in soils to increase the bioavailability of heavy metals and enhance the efficiency of phytoremediation (Luo et al., 2006; Attinti et al., 2017). EDDS can affect soil minerals, soil physical structure, microbial communities, enzymatic activity, and the stability of SOM (Luo et al., 2015). However, previous studies primarily focused

* Corresponding author.
** Corresponding author.
E-mail addresses: prguo@fenxi.com.cn (P.-r. Guo), chenzhiliang@scies.org (Z.-l. Chen).

https://doi.org/10.1016/j.envres.2024.120085
Received 23 August 2024; Received in revised form 27 September 2024; Accepted 27 September 2024
Available online 29 September 2024

on the extraction efficiency of EDDS on heavy metals, while the impacts of EDDS on the preservation of soil C have been rarely studied. To mitigate the climate warming, it is worth paying more attention on the variation of SOM stability and carbon emission during soil remediation. A better understanding of soil C turn over in EDDS-assisted phytoremediation is urgently needed.

Soil organic matters (SOM) are largely adsorbed on minerals (e.g., goethite, hematite, and gibbsite) through ligand exchange, electrostatic attraction, or oxide-cation bridging (Yao et al., 2019; Li et al., 2021). Previous studies have revealed that EDDS causes soil mineral dissolution by complexing with Fe, Al or Ca from metal oxides (Tsang et al., 2009; Beiyuan et al., 2017). With the dissolution of minerals or the destruction of organic-metal linkages, organic matter is prone to being released into aqueous solution, forming the dissolved organic matter (DOM) (Tsang et al., 2007; Yip et al., 2009). However, the dissolution of SOM induced by EDDS is predominantly observed during EDDS-assisted soil flushing or washing, wherein the soil-solution ratio, EDDS dosage, and reaction modes notably vary from those in *situ* EDDS-assisted phytoremediation. Whether and to what extent EDDS influences the SOM stability and DOM pool in phytoremediation is uncertain. Besides, the interactions among EDDS, plant roots, and microbes are complex in the rhizosphere of plants. EDDS potentially affects the stability of SOM by altering the microbial growth and activities (Yang et al., 2013; Fang et al., 2017). In addition, plant respiration may affect the transport and distribution of EDDS in rhizosphere (Zhao et al., 2020). The connection between EDDS, roots, microbes, and soil C in the plant rhizosphere during phytoremediation remain unclear.

DOM, as the most mobile and active fraction of soil, plays a crucial role in soil C turnover (Sheng et al., 2023). DOM is particularly susceptible to decomposition by microbes or leaching with runoff (Gan et al., 2021). Therefore, the increase in soil DOM resulting from certain treatments suggests the destabilization of SOM. Soil DOM is an organic mixture with extreme complexity that contains thousands of molecules. The change in DOM composition, particularly at the molecular level, provides a window to observe the process of organic matter turnover in soil (Wu et al., 2023). Yet, little is known about how EDDS affects the preservation of soil C through the disturbance of the DOM pool. In recent years, the rapid development of electrospray ionization Fourier transform ion cyclotron resonance mass spectrometry (ESI-FT-ICR MS) provides a good opportunity to analyze the molecular composition of DOM. ESI-FT-ICR MS have been demonstrated to be effective to identify thousands of individual DOM formulae simultaneously (Perminova et al., 2014; Qi et al., 2022). The understanding of DOM transformation at the molecular level is crucial for gaining a comprehensive insight into the stability of soil C and the mechanisms of potential C loss during EDDS-assisted phytoremediation. Thus, practical recommendations can be provided to engineers to develop the win-win phytoremediation strategies that are effective in removing both heavy metal pollution and reducing C emission.

Therefore, the objectives of this work were to investigate the impacts of EDDS on the quantity and molecular composition of rhizosphere soil DOM during EDDS-assisted phytoremediation and to elucidate the underlying mechanisms. Ryegrass is selected as a representative plant due to its fast growth rate, high tolerance to heavy metals, and frequent use in conjunction with EDDS in phytoremediation. Ryegrass was grown in a multi-interlayer rhizobox to separate the rhizosphere and non-rhizosphere soils. ESI-FT-ICR MS is employed together with conventional three-dimension excitation emission matrix (EEM) spectroscopy to acquire molecular information and optical properties of soil DOM.

2. Materials and methods

2.1. Soil sampling and materials

Soil samples used for phytoremediation experiments were collected from an abandoned Cu mine in the town of Tangshan (32°03′N, 118°47′W) in Nanjing, Jiangsu, China. The physiochemical properties of polluted soils were analyzed according to Cater and Gregorich (2006) and the results were as follows: the pH ($CaCl_2$) of 7.72, sand/silt/clay of 32%/47%/21%, total organic carbon of 18.6 g kg^{-1}, total organic nitrogen of 1.72 g kg^{-1}, total Cd, Cu, Pb and Zn of 1.72, 805, 67.2, and 230 mg kg^{-1}, respectively and total Fe, Ca, and Al of 40.8, 18.6, and 39.1 g kg^{-1}, respectively.

A multi-interlayer rhizobox was used for plant growth (Fig. S1), which was separated into six compartments by the nylon mesh (<25 μm). Ryegrass seedlings were planted in the leftmost compartment (rhizosphere) of the multi-interlayer rhizobox. Plant roots cannot penetrate through the nylon mesh, but soil solution was able to transport between the compartments. The leftmost compartment (2 cm) was rhizosphere, and the adjacent five compartments were non-rhizosphere soils with different distances (0–1, 1–2, 2–3, 3–4, 4–6 cm) to rhizosphere. A total of 240-, 120-, 120-, 120-, 120- and 240-g soils were packed into six compartments from rhizosphere to non-rhizosphere compartments.

2.2. Incubation experiment

Ryegrass seeds were sterilized (95% ethanol), washed, and germinated for seven days. Rygrass seedlings were cultivated in the rhizobox under controlled conditions of temperature, relative humidity and photoluminescence (25 °C/60%/325 μmol photons m^{-2} s^{-1}/16 h day and 20 C/60%/0 μmol photons m^{-2} s^{-1}/8 h night) in a climate growth chamber. The soil moisture in rhizoboxes was kept at 60% maximum water holding capacity by supplementing deionized water periodically. After three weeks, 120 mM EDDS (Na_3-S,S-EDDS, Sigma-Aldrich, Germany) was added to the rhizobox from the top of soil surface to achieve a dosage of 5 mM kg^{-1}. A group of rhizoboxes treated by the same amount of deionized water as EDDS-containing solution was set as control. A group of rhizoboxes with the same treatment of EDDS but without plant growth was set as another control. Each rhizobox group with or without EDDS treatment had three replicates.

After EDDS treatment for 7 d, the aboveground parts of ryegrass were removed from rhizoboxes and fresh soils were collected from rhizosphere and non-rhizosphere compartments. Plant roots were carefully removed from the rhizosphere soils (Fig. S1). Soils were collected from each compartment of the rhizobox destructively.

Plant roots and shoots were separated, washed and oven-dried at 105 °C for 48 h before the dry weight were recorded. Root and shoot samples were ground and digested with 4:1 (v/v) concentrated HNO_3 and $HClO_4$. The concentrations of heavy metals (Cd, Cu, Pb, Zn) in plant digest were measured by inductively coupled plasma-mass spectrometry (ICP-MS, Agilent 7700 series). Soil moisture was determined by weighing fresh and dried soil at 105 °C for 48 h.

EDDS remaining in soils was extracted from 1 g freeze-dried soils using 10 ml deionized water for 2 h. EDDS in filtered solution was derivate to FeEDDS and analyzed by high performance liquid chromatography system equipped with an Ultraviolet–Visible (UV–vis) detector (HPLC-UV, Waters 2487) and a reversed-phase C18 column (259 × 4.6 mm, 5 μm) (Inertsil ODS-3, Shimadzu, Japan) (Katata et al., 2006; Zhao et al., 2020). The eluent for the FeEDDS method consisted of methanol and 0.02 M tetrabutylammoniumbromide (10:90, v:v) at pH 4.0, applied at a flow rate of 1 mL min^{-1} in the isocratic elution mode.

Total dissolved organic carbon (TDOC) and total dissolved nitrogen (TDN) were extracted from fresh soils with deionized water at a ratio of 1:10 (w:v) on a dry weight soil basis for 2 h, filtered (0.45 μm) and analyzed by automated TOC/TN Analyzer (Shimadzu). The NH_4^+ and NO_3^- from soil extracts were analyzed by a portable colorimeter (DR890, Hach) (Cater and Gregorich, 2006). Soil DOC was the difference between TDOC and EDDS-C. Soil DON was calculated by subtracting EDDS-N, NO_3^--N and NH_4^+-N from TDN, as NO_2^--N was negligible. Soil available P was extracted by $NaHCO_3$ and analyzed by molybdenum antimony resistance-colorimetry (Margesin and Schinner, 2005). The

dissolved heavy metals and mineral cations (Cd, Cu, Pb, Zn, Fe, Mn, Ca, Mg and Al) in soil extracts were measured by ICP-MS.

2.3. Analysis of soil microbial biomass C/N and enzyme activities

Microbial biomass carbon and microbial biomass nitrogen were measured by the chloroform fumigation-K_2SO_4 extraction method (Vance et al., 1987). Five grams (dry weight) of fresh soil samples were placed in a vacuum desiccator containing a small amount of NaOH, water, and ethanol-free chloroform. After evacuating the air to maintain the chloroform boiling for 3–5 min, transfer the desiccator to fumigate the soil under dark at 25 °C for 24 h. Evacuate again to completely remove chloroform from the soil. The fumigated soil and non-fumigated blanks were extracted by 0.5 M K_2SO_4 with a ratio of 5:1 (w:v). The organic carbon and total nitrogen content in the extraction solutions were measured by a TOC/TN Analyzer. The microbial biomass carbon and nitrogen are calculated by dividing the difference in organic carbon and nitrogen content between fumigated and non-fumigated soil samples by the conversion factor (0.45) (Vance et al., 1987).

Soil urease activity was measured using the indophenol blue colorimetric method, with urea as a substrate, and quantified with a spectrophotometer at 578 nm (Guan, 1986). Soil saccharase activity was determined using the 3,5-dinitrosalicylic acid colorimetric method, with sucrose as the substrate, and quantified at 508 nm (Guan, 1986). Acid phosphatase activity was measured using the p-nitrophenyl phosphate colorimetric method and quantified at 400 nm (Eivazi and Tabatabai, 1977; Dick, 2011).

2.4. Analysis of optical and molecular characterization of soil DOM

To extract DOM, deionized water was added to soil at solid-solution ratio of 1:10 (w:v). The mixture was shaken on an end-over-end rotator (12 h at 30 rpm at 20 °C), centrifuged (4000 rpm for 10 min), filtered (0.45 μm) and stored at 4 °C for further analysis.

Three-dimension excitation emission matrix (3D-EEM) spectra of soil DOM were recorded using a spectrofluorometer (Aqualog, Horiba). All soil extracts were diluted to ~7–8 mg/L of DOC before analysis, to ensure the absorbance at 254 nm < 0.3 and minimize the inner filter effects (Ohno, 2002). The 3D-EEM spectra were scanned in excitation (Ex) range of 240–600 nm with an increment of 3 nm and emission (Em) range of 213.033–619.454 nm with an increment of 1.64 nm. The integration time of the measurements was 1 s according to the fluorescence intensity of samples. The DrEEM toolbox in MATLAB was used to remove the first and second Rayleigh and Raman Scatter from EEM spectra and normalized to Raman units (RU). The PARAFAC modeling was performed to excavate fluorescence components by non-negativity constraints, residual analysis, split-half analysis, and visual inspection (Stedmon and Bro, 2008). The relative percentages of the individual fluorescent components were estimated by their maximum fluorescence intensity (Fmax). The parameters, including fluorescence index (FI), biological index (BIX) and humification index (HIX), were calculated by equations shown in Supporting Information (SI) (Wang et al., 2022b; Yi et al., 2023).

Soil DOM from rhizosphere and non-rhizosphere (3–4 cm) were selected for molecular characterization by electrospray ionization coupled to Fourier transform ion cyclotron resonance mass spectrometry (ESI-FT-ICR MS, Bruker Daltonics Solarix XR 7.0T). Before ESI-FT-ICR MS analysis, DOM extracts from three soil repeats were combined, desalinated, and concentrated by solid-phase extraction (SPE) with styrene-divinyl-benzene polymer cartridges (Varian Bond PPL Elute, 1 g per 6 mL). The SPE procedures were as follows: 1) DOM extracts were acidified to pH = 2 by HCl; 2) 12 mL HPLC methanol and 12 mL acidified ultrapure water (pH = 2) were passed through cartridges for clean-up; 3) acidified DOM extracts were passed through the PPL cartridges via vacuum pump; 4) 18 mL acidified ultrapure water was passed through cartridges to remove salts; 5) cartridges were dried with N_2 gas for 10 min to eliminate the interferences of residual HCl and water to measurement; 6) DOM was collected from the cartridges using 2 mL of HPLC methanol (Dittmar et al., 2008; Gan et al., 2021). DOM elutes of stored at −20 °C in dark prior to ESI FT-ICR MS measurement. The recovery rate of DOM in SPE treatment ranges from 57.3% to 79.8%. The reference Suwannee River natural organic matter (SRNOM 2R101N) obtained from the International Humic Substances Society was used as quality control.

Soil DOM elutes obtained above were diluted with ultrapure water to give a final sample composition of 1:1 (v:v) methanol:water with DOC about 25 mg/L for analysis on the FT-ICR MS. Samples were continuously infused into the electrospray ionization (ESI) unit using a Hamilton syringe at a flow rate of 2 μL/min. Samples were ionized by ESI in negative ion mode. The electrospray voltage was kept at 4000 V. Mass spectra were acquired over 300 scans with an ion accumulation rate time of 0.1 s and a m/z of 150–800. The instrument was externally calibrated with sodium trifluoroacetate. Sample spectra were internally calibrated with Suwannee River fulvic acid, and the mean square errors of internal calibration were <0.2 ppm. PPL extraction blanks were analyzed together with soil DOM samples to check contamination and peaks from blanks were removed from sample spectra. Molecular formula were assigned to peaks with signal-to-noise ratio >6 using the TRFu code written by Fu et al. (2020) in MATLAB. The tolerance of mass error of a given peak between measured mass and theoretical mass was set to 1.0 ppm. The aromaticity index (AI_{mod}), double bond equivalent (DBE) and nominal oxidation state of carbon (NOSC) were calculated based on each molecular formula according to equations shown in SI. The average values of m/z, C, H, O, N, S, P, AI_{mod}, DBE and NOSC were calculated using the intensity-weighted method. The van Krevelen (VK) diagram was constructed and divided into seven chemical groups based on the ratio of hydrogen to carbon (H/C) and ratio of oxygen to carbon (O/C): 1) lipids (O/C = 0–0.3, H/C = 1.5–2.0), 2) proteins and amino sugars (O/C = 0.3–0.67, H/C = 1.5–2.2), 3) carbohydrates (O/C = 0.67–1.2; H/C = 1.5–2.4), 4) unsaturated hydrocarbons (O/C = 0–0.1, H/C = 0.7–1.5), 5) lignins (O/C = 0.1–0.67, H/C = 0.7–1.5), 6) tannins (O/C = 0.67–1.2, H/C = 0.5–1.5), and 7) condensed aromatics (O/C = 0–0.67, H/C = 0.2–0.7) (Trainer et al., 2021; Han et al., 2022; Huang et al., 2022).

2.5. Statistical analysis

The significance of differences between the means of two groups was evaluated by the Dunnett (two-sided) post-hoc test (*P < 0.05 and **P < 0.01) using SPSS 19.0. The one-way analysis of variation (ANOVA) was performed to assess the differences between multiple groups using the Duncan Test at a significance level of 0.05. Association between multiple biochemical parameters was analyzed using Pearson's correlation analysis. The partial least squares path modeling (PLS-PM) was conducted using package "plspm" of R 4.3.1 to reveal the causal relationships among the latent variables. The model performance was evaluated by the goodness of fit index.

3. Results and discussion

3.1. Distribution of EDDS in the rhizobox and influence on phytoremediation efficiency

EDDS-containing solution was evenly added to each compartment of the multi-interlayer rhizobox with care, and its distribution in rhizobox after 7 d is shown in Fig. 1a. Compared to the initial dosage (5 mmol kg^{-1}), 81.8% and 84.6% of EDDS remained in planted and unplanted rhizoboxes, respectively. EDDS was evenly distributed in each compartment of unplanted rhizobox, while EDDS was highly accumulated in the rhizosphere and its concentration decreased with the increasing distance from rhizosphere in the planted rhizobox. The contrasting distribution pattern of EDDS in planted and unplanted

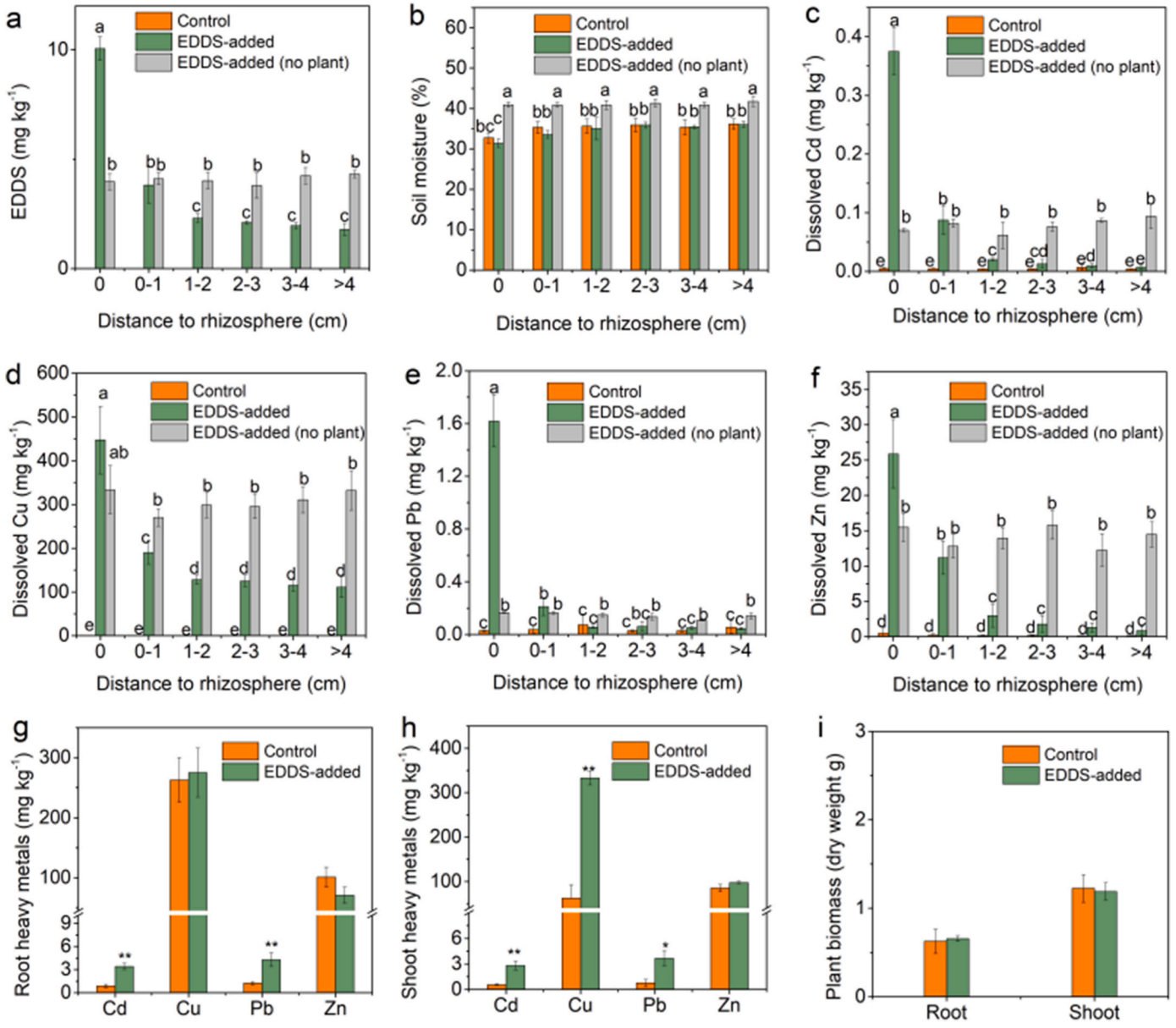

Fig. 1. EDDS concentration (a), soil moisture content (b), dissolved heavy metals (c–f) in rhizobox soils, and concentrations of heavy metals in ryegrass root (g) and shoot (h) as well as plant biomass of ryegrass (i). (Different letters indicate significant differences across treatments according to Duncan's test at $P < 0.05$, * and ** represent significant difference by Dunnett's test at $P < 0.05$ and $P < 0.01$, respectively).

rhizoboxes suggested the horizontal transport of EDDS from the far-rhizosphere to the rhizosphere of ryegrass in the planted rhizobox. As supported by the content of soil moisture (Fig. 1b), dense ryegrass roots (Fig. S1) created a water potential gradient in surrounding soils and thus drove the transport of soil solutions containing soluble EDDS from the far-rhizosphere to near-rhizosphere and rhizosphere (Tang et al., 2023).

After application of EDDS, the concentrations of dissolved Cd, Cu, Pb and Zn in soils increased by 0.46–80.5, 208–643, 0–56.2, and 5.5–51.3 folds respectively (Fig. 1c–f). The concentrations of dissolved heavy metals in the rhizosphere were much higher than that in the non-rhizosphere. This can be due to the more intense extraction of heavy metals by the higher concentration of EDDS in the rhizosphere than the non-rhizosphere (Yang et al., 2012; Luo et al., 2015), as well as the transport of soluble metals from the non-rhizosphere to rhizosphere. With the significant increase of soluble heavy metals in the rhizosphere following the application of EDDS, the concentrations of Cd and Pb in ryegrass roots increased by 2.86 and 2.50 folds, respectively (Fig. 1g), and the concentrations of Cd, Cu, Pb and Zn in shoots increased by 5.09, 5.34, 4.75, and 1.14 folds, reaching 2.82, 333, 3.66 and 97.4 mg kg^{-1}, respectively (Fig. 1h). The translocation factor (TF), indicating the translocation efficiency of heavy metals from root to shoot, was calculated as the ratio of shoot to root heavy metals. EDDS increased the TF of Cd, Cu, Pb and Zn by 31.8%, 410%, 36.0%, and 62.7%, respectively. EDDS exhibited better performance on facilitating phytoremediation of Cu compared to other metals, which was probably correlated with the higher affinity between EDDS and Cu, as well as the presence of more available Cu for EDDS extraction in soils (Wang et al., 2022a). In addition, EDDS showed no inhibition effects on ryegrass growth (Fig. 1i). Therefore, the application of EDDS effectively solubilized heavy metals (particularly for Cu) from soils, and increased the uptake and translocation of heavy metals from root to shoot.

3.2. Influence of EDDS on DOM quantity in the rhizosphere and non-rhizosphere

To study the variation in stability of SOM after EDDS-assisted phytoremediation, the concentrations of DOC and DON were investigated in the rhizobox. By excluding the contribution of C and N from exogenous EDDS itself, it is seen that the application of EDDS led to the obvious increase of average soil DOC by 180% and DON by 627% in the planted rhizobox (Fig. 2a and b), which can be interpreted by the partial degradation of EDDS or dissolution of SOM. In consideration of that the added EDDS can be transformed to *N*-(2-aminoethyl)aspartic acid, then to ethylenediamine, and finally to NH_4^+ and CO_2 (Chen et al., 2010). The degradation of EDDS in the planted rhizobox at most contributed 19.1% to the changes of DOC and 37.8% for DON, when no EDDS was mineralized. Therefore, instead of EDDS degradation, SOM dissolution should be the major reason responsible for the substantial changes of soil DOC and DON after EDDS application. After such a short application period, the content of SOM dissolved by EDDS at least accounted for 2.10% of the total. So, the issues of SOM dissolution induced by EDDS deserves more attention in practice. In contrast to DOC/DON, the concentration of available P in soils was not affected by EDDS (Fig. 2c), indicating that the newly dissolved organic matter contains few P.

The mobilization of SOM can be caused by the dissolution of Fe-, Al- or Ca-oxides induced by EDDS, as these minerals are important soil components for organic matters adsorption via ligand exchange, cation bridge, van der Waals and hydrogen bond (Yip et al., 2009; Begum et al., 2020). In this study, SOM dissolution largely relied on the dissolution of soil Fe and Al (Fig. 2d and e) instead of Ca (Fig. 2f), as evidenced by the remarkable increase of dissolved Fe by 3.47–60.2 folds and dissolved Al by 3.14–5.31 folds in EDDS-added soils. In particular, EDDS can destabilize the Fe-O bond formed between iron oxides and organic matters, complex with Fe through ligand exchange reactions, and then release the adsorbed organic matters to soil solutions (Komárek et al., 2009; Han et al., 2021). In addition, DOC/DON showed increasing trends with the decrease of distance to rhizosphere, which is probably due to the more intensive dissolution of soil mineral and organic matters induced by the higher concentration of EDDS in rhizosphere and near-rhizosphere. On the other hand, the transport of solubilized organic matters through the water potential gradient can also contribute to the higher concentrations of DOC/DON in rhizosphere.

3.3. Influence of EDDS on microbial biomass and enzyme activities in the rhizosphere and non-rhizosphere

Soil microbes play an important role in decomposition and mineralization of SOM, and thus the microbial biomass C/N and enzyme activities in the rhizobox were investigated (Li et al., 2023). As shown in Fig. 3, the microbial biomass carbon (MBC) and microbial biomass nitrogen (MBN) increased by 3.04–43.9% and 48.0–290%, respectively, in EDDS-added soils compared to control (Fig. 3a and b), and they showed strong positive correlation with EDDS ($r = 0.84$ for MBC, and $r = 0.96$ for MBN). Similarly, Wang et al. (2018) also reported increased microbial biomass in EDDS-added soils. The biodegradable EDDS itself probably provided fresh C and N-source and stimulate microbial growth rapidly, as evidenced by the increase of soil mineral N (Table S1) (Yang et al., 2013; Fang et al., 2017). Furthermore, soil microbes can also gain additional nutrients that released from the dissolution of SOM caused by EDDS application (Kaurin et al., 2020).

Urease can catalyze the hydrolysis of urea and some amides, which is associated with N-cycling microbes (Tu et al., 2020). Compared to control, EDDS enhanced urease activities by 29.4% in rhizosphere but showed no effects in non-rhizosphere (Fig. 3c). Beiyuan et al. (2017) also measured an increase of urease activities in EDDS-washed soils, but Ju et al. (2020) found no effect of EDDS on urease activities in

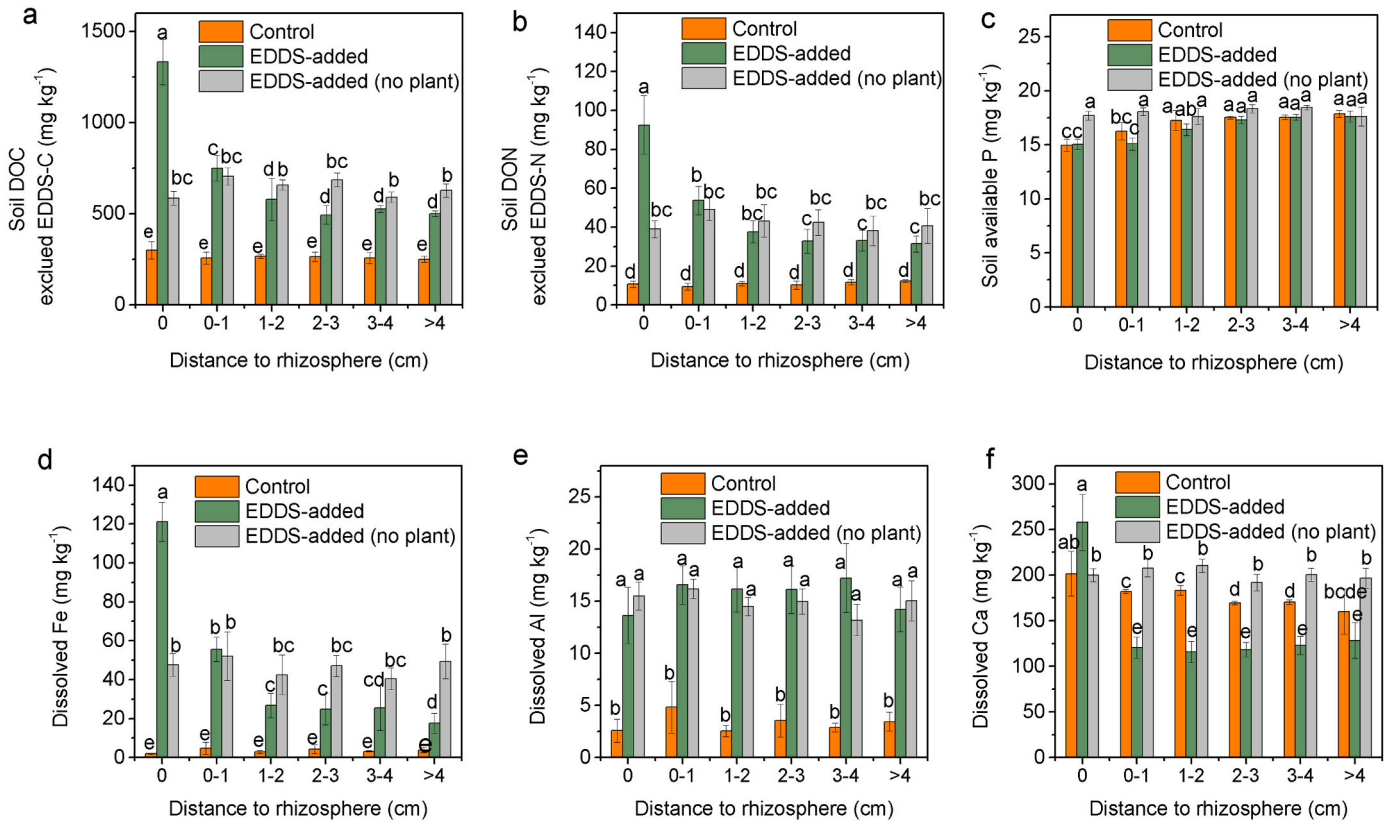

Fig. 2. Concentrations of soil DOC (exclude C from EDDS) (a), soil DON (excluded N from EDDS) (b), available P (c), dissolved Fe (d), dissolved Al (e), and dissolved Ca (f) in rhizobox soils with/without EDDS application. (Different letters indicate significant differences across treatments according to Duncan's test at $P < 0.05$).

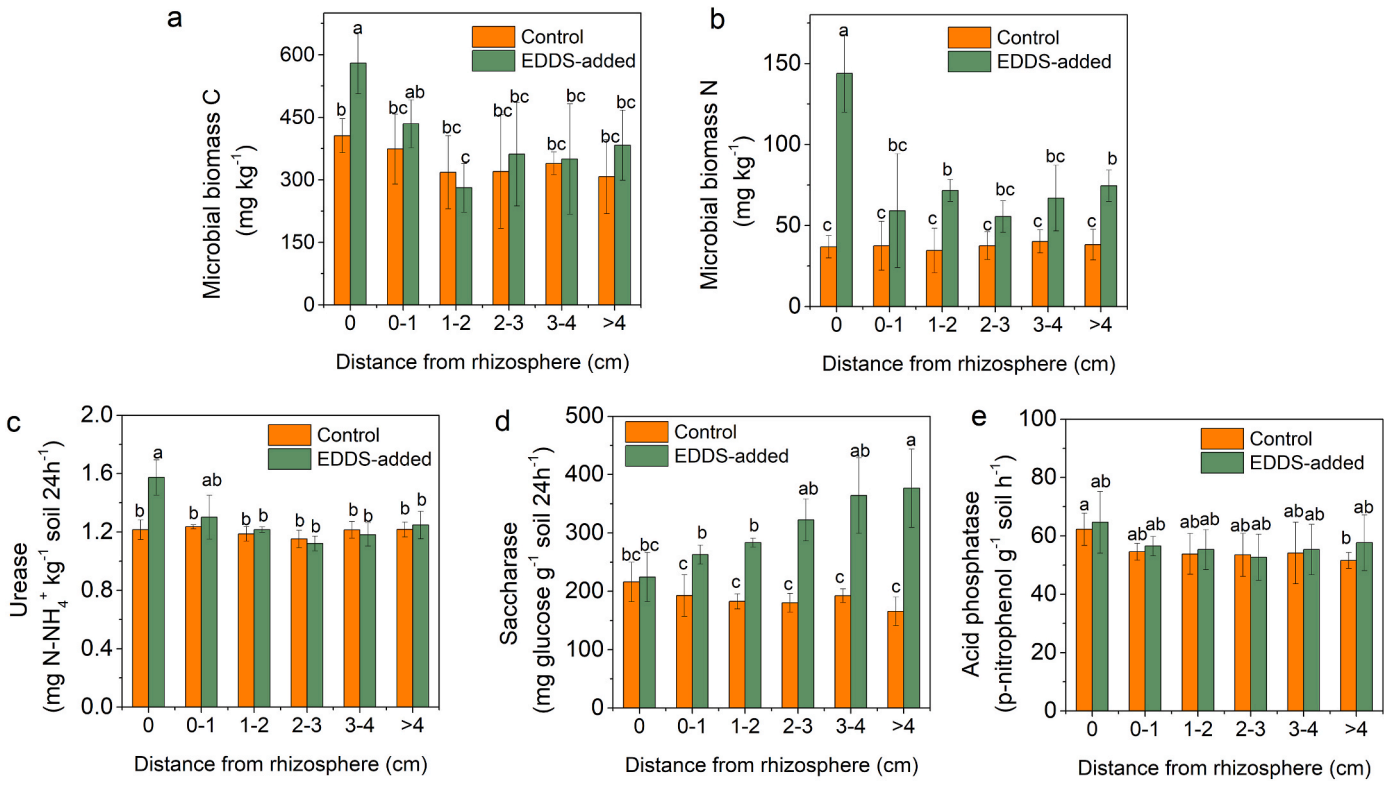

Fig. 3. Concentrations of microbial biomass C (a) and microbial biomass N (b), and activities of urease (c), saccharase (d), and acid phosphatase (e) of soils from rhizobox with/without EDDS application. (Different letters indicate significant differences across treatments according to Duncan's test at $P < 0.05$).

phytoremediation. The different response of urease activities in rhizosphere and non-rhizosphere can be correlated to the concentration of EDDS in soils. Saccharase can hydrolyze sucrose to monosaccharide and reflects the activities of soil microbes on soil C decomposition (Xu et al., 2023). EDDS application generally increased saccharase activities, but the increment extent of saccharase activities decreased from 127% to 0.04% with the decrease of distance to rhizosphere (Fig. 3d). The decreased effects of EDDS on saccharase activities in rhizosphere and near-rhizosphere could be correlated to the toxicity of increased solubilized heavy metals (Fig. 1c–f) (Ju et al., 2020). Soluble heavy metals impair saccharase activities in soils, so the promotion effects of EDDS on saccharase were probably compromised by the inhibition effects of elevated soluble Cd, Cu, Pb and Zn in rhizosphere and near-rhizosphere (Han et al., 2020). Acid phosphatase helps organic phosphorus to mineralize and produce inorganic phosphorus (Chen et al., 2023). EDDS exhibited no significant impacts on the activities of acid phosphatase (Fig. 3e), as supported by the findings that EDDS did not affect the available P of soils (Fig. 2c).

3.4. *Influence of EDDS on fluorescence composition of soil DOM in the rhizosphere and non-rhizosphere*

The characteristic of soil DOM composition reflects its bioavailability and potential to be mineralized. However, to our knowledge, the impacts of EDDS on the composition of soil DOM have been rarely studied. Herein, the fluorescence composition of soil DOM after EDDS application was recorded by 3D-EEM, and the spectral parameters are listed in Table 1. HIX is a measure of the complexity and the aromatic nature of DOM (Santana-casiano et al., 2022). EDDS application increased HIX by 93.3%–41.6% from rhizosphere to non-rhizosphere, indicating the increment of high-molecular-weight aromatics in DOM. BIX reflects the proportion of newly and microbially produced DOM (El-naggar et al., 2020). FI indicates the allochthonous or autochthonous source of DOM (Wang et al., 2022b). The values of BIX and FI had no significant

Table 1
Fluorescence indices of DOM in rhizobox soils with/without EDDS application.

Distance from rhizosphere (cm	FI	HIX	BIX	C1%	C2%	C3%
Control						
0	1.5 ± 0.0a	8.1 ± 0.9c	0.5 ± 0.0a	44 ±2c	30 ±2a	26 ±2a
0–1	1.5 ± 0.0a	9.2 ± 0.9bc	0.5 ± 0.0a	44 ±1c	32 ±1a	24 ±2a
1–2	1.4 ± 0.0b	9.8 ± 0.7bc	0.5 ± 0.0a	45 ±2bc	30 ±3a	25 ±3a
2–3	1.4 ± 0.0 ab	10.1 ± 2.0bc	0.5 ± 0.0a	45 ±1c	32 ±1a	23 ±2a
3–4	1.4 ± 0.0 ab	10.2 ± 1.1bc	0.5 ± 0.0a	46 ±2bc	34 ±1a	21±2 ab
4–6	1.4 ± 0.1 ab	10.3 ± 0.9b	0.5 ± 0.0a	43 ±2c	32 ±2a	25 ±2a
EDDS-added						
0	1.5 ± 0.0a	15.6 ± 3.8a	0.5 ± 0.0a	55 ±3a	34 ±2a	11 ±1d
0–1	1.5 ± 0.0a	15.1 ± 1.3a	0.5 ± 0.0a	53 ±3a	32 ±2a	14 ±1c
1–2	1.5 ± 0.0a	14.7 ± 2.1a	0.5 ± 0.0a	50±2 ab	34 ±1a	16 ±1bc
2–3	1.5 ± 0.0a	14.6 ± 2.0a	0.5 ± 0.0a	50±1 ab	32 ±1a	18 ±1b
3–4	1.5 ± 0.0a	14.7 ± 1.5a	0.5 ± 0.0a	49 ±3b	34 ±1a	18 ±2bc
4–6	1.5 ± 0.0a	14.5 ± 1.9a	0.5 ± 0.0a	51±2 ab	33 ±2a	16 ±2bc

variation after EDDS application. Furthermore, to understand the compositional changes of 3D-EEM spectra of soil DOM, PARAFAC modelling was used to extract fluorescent components from the complex matrix. Three fluorescent components were identified (Fig. 4), including C1 ($\lambda_{Ex/Em}$=<250(314), 417), C2 ($\lambda_{Ex/Em}$ = 260(366), 492) and C3 ($\lambda_{Ex/Em}$ = 266, 417). By comparing these fluorescent components to

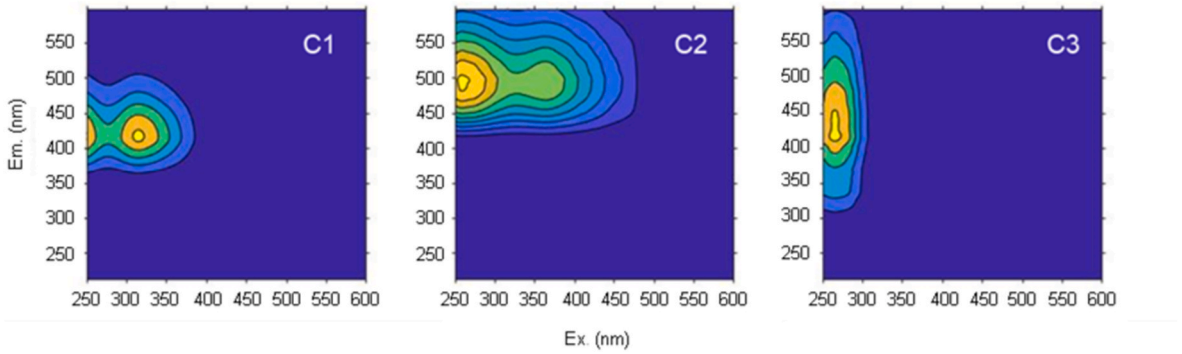

Fig. 4. Contour plots of the three components identified using the EEM-PARAFAC in all soil extracts.

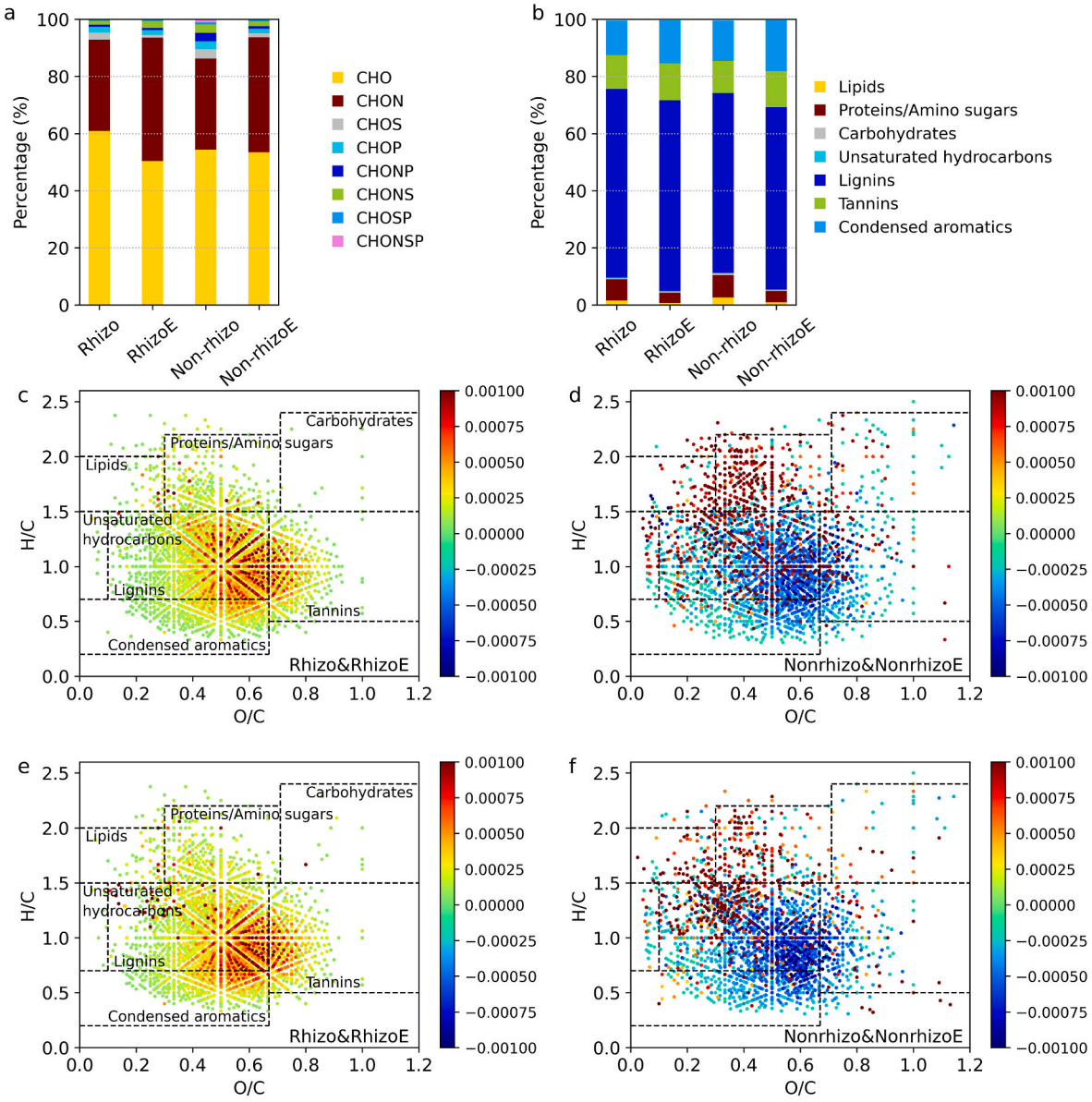

Fig. 5. Comparision of DOM formulae between soils with/whitout EDDS application. Percentage of different element groups and organic components of formulae in control (a) and EDDS-added soil (b). Van Krevelen (VK) diagrams of shared formulae (unchanged DOM) beteween control and EDDS-added soil from rhizosphere (c) and non-rhizosphere (e). The color bar refers to the relative intensity normalized to the sum of all assigned peaks. The difference in formulae between control and EDDS-added soil from rhizosphere (d) and non-rhizosphere (f). Red dot: unique DOM speicies in control soil (degraded DOM). Blue dot: unique DOM speicies in EDDS-added soil (newly formed DOM).

OpenFluor library, C1 and C2 referred to humic-like substance with high molecular weight, and C3 resembled to humic-like substance with low molecular weight (Ishii and Boyer, 2012; Mostofa et al., 2019). After application of EDDS, the percentage of C1 increased by 25.0%–18.6%, and the percentage of C3 decreased by 57.7%–36.0% from the rhizosphere to non-rhizosphere (Table 1), revealing that EDDS led to the high molecular weight humic-like substance prevail in DOM pool. Breaking of Fe/Al bridges by EDDS can cause the detachment of OM-Fe or OM-Al complex and promote the release of C1 (Piccolo and Drosos, 2024).

3.5. Influence of EDDS on molecular composition of DOM in the rhizosphere and non-rhizosphere

The molecular signature of rhizosphere and non-rhizosphere DOM were investigated by ESI-FT-ICR MS. In the control group, a total of 5739 and 4618 formulae were identified in rhizosphere and non-rhizosphere soils, respectively. In the EDDS-added group, a larger number of formulae (7569 and 6191) were detected, indicating that EDDS heightened the molecular chemodiversity of soil DOM. EDDS-induced alterations in molecular characteristic parameters of soil DOM were observed (Table S2). The parameter DBE reflects the double bond structure of DOM (Lv et al., 2016), and the average DBE_{wt} increased by 7.04% and 7.60% in EDDS-added rhizosphere and non-rhizosphere soils compared to those in control soils. Similarly, the average AI_{mod} representing aromatic structures showed a slight elevation (Wang et al., 2020). Both aromatic ($0.5 < AI_{mod} < 0.67$) and condensed aromatic ($AI_{mod} > 0.67$) compounds exhibited increments by 39.5–42.1% and 54.7–60.0% in EDDS-added rhizosphere and non-rhizosphere soils, respectively. This suggests that EDDS increased the presence of polyphenols and condensed aromatics in DOM, aligning with the EEM results that indicated higher HIX values in EDDS-added soils compared to control soils.

To investigate the alteration of EDDS on soil DOM composition, the thousands of compounds in each sample were grouped into eight categories according to their elemental composition (Fig. 5a). CHO and CHON emerged as the predominant compounds, constituting 86.3–93.7% of all samples. EDDS induced a notable increase in the percentages of CHON compounds in both rhizosphere (from 31.9% to 43.2%) and non-rhizosphere (from 31.9% to 40.3%), while the proportions of CHO compounds exhibited corresponding decreases from 60.9% to 50.4% in rhizosphere and from 54.3% to 53.4% in non-rhizosphere. The elevation in CHON compounds agrees with the more substantial increase in DON compared to DOC following EDDS application (Fig. 2). Utilizing the characteristic ratios of H/C and O/C in molecular formulae, the compounds in each sample were classified into seven biogeochemical classes of DOM (Fig. 5b and c). After applying EDDS, tannin-like compounds increased by 9.11% and 11.3% in the rhizosphere and non-rhizosphere, respectively. Meanwhile, condensed aromatics-like compounds increased by 24.4% and 26.5%, respectively. In contrast, lipid-like compounds decreased by 56.3% and 63.9% in the rhizosphere and non-rhizosphere, and proteins/amino sugars-like compounds decreased by 52.1% and 49.5%, respectively. In summary, EDDS led to an augmentation in CHON, tannins-, and condensed aromatics-like compounds, accompanied by a reduction in CHO, proteins-, and amino sugar-like compounds in the DOM pool. The degree of molecular transformation of DOM in the rhizosphere surpassed that in the non-rhizosphere, aligning with the higher concentration of EDDS observed in the rhizosphere.

To gain insight into the transformation of soil DOM during EDDS-assisted phytoremediation, three categories of formulae-unchanged, degraded and newly formed-were identified by comparing DOM formulae in the control and EDDS-added groups (Fig. 5c–f). The control and EDDS-added soils shared 4971 (rhizosphere) and 4038 (non-rhizosphere) formulae in common, which were considered as unchanged DOM species affected by EDDS (Fig. 5c–e). They were mainly lignins-like compounds. In contrast, 766 and 613 unique formulae were observed in the control but lost in the EDDS-added group. These compounds, mainly CHO compounds belonging to lipids-, proteins/amino sugars-, and lignins-like compounds, are susceptible to degradation by soil microbes (Fig. 5d–f) (Gong et al., 2022). As indicated earlier (Fig. 3), EDDS heightened soil microbial biomass and enzyme activities, potentially accelerating the microbial consumption of these bioavailable DOM compounds. Additionally, 2596 and 2152 formulae, exclusively observed in EDDS-added rhizosphere and non-rhizosphere soils and absent in the control, were designated as newly formed DOM species (Fig. 5d–f). They were N-rich compounds that mostly belonged to the lignins-like compounds with high O/C ratios, tannins- and condensed aromatics-like compounds that were typically recalcitrant (Gu et al., 2023). The newly formed DOM can originate from microbial metabolites, or dissolved SOM induced by EDDS as mentioned above. Therefore, EDDS probably shifted the molecular composition of DOM pool by promoting the degradation of bioavailable DOM, production of microbial metabolites, or releasing recalcitrant SOM from soil minerals.

The degraded molecules represent the bioavailable DOM (BDOM), while the newly formed molecules refer to the recalcitrant DOM (RDOM). The molecular transformation pathways of BDOM to RDOM in the rhizosphere and non-rhizosphere, induced by EDDS, were further analyzed by Kendrick mass defect from the perspective of homologs (Fig. 6). Homologous series with different numbers of functional groups (e.g. $-CH_2$, $-H_2$, -HOH, -COO, -OO, $-CH_2O$) can be identified by KMD analysis because they have the same KMD values. At a specific given KMD value, the number of functional groups increases with the nominal Kendrick mass. The homologs of degraded DOM from the rhizosphere or non-rhizosphere had more hydrogen-containing functional groups of $-CH_2$, $-H_2$ and HOH (Fig. 6a–c, g-i) particularly in the m/z range of 250–500, compared to those of newly formed DOM, suggesting that EDDS promoted the microbial degradation of BDOM through chain scission and dehydration (Gu et al., 2023). Besides, the homologs of newly formed DOM from rhizosphere or non-rhizosphere had more functional groups of -COO, and -OO (Fig. 6d,e,j,k). As such, the RDOM molecules can be formed through carboxylation and hydroxylation (Gu et al., 2023). Overall, the application of EDDS can accelerate the microbial mineralization of BDOM through chain scission and dehydration, and the formation of RDOM through carboxylation and hydroxylation.

3.6. Potential mechanisms underlying SOM destabilization induced by EDDS

According to our rhizobox study, the application of EDDS increased soil DOC/DON levels and facilitated the biotransformation of DOM in the ryegrass rhizosphere during EDDS-assisted phytoremediation. With the use of partial least squares path modeling (PLS-PM) and correlation analysis (Fig. 7a and b), a conceptual model was developed to explain the mechanisms that destabilize SOM due to the presence of EDDS (Fig. 7c). When applying the highly soluble EDDS to soils, it was transported quickly toward plant roots, probably through the water potential gradient in the rhizosphere. The transport of EDDS from the far-rhizosphere to the rhizosphere exacerbated the extent of SOM destabilization in the plant rhizosphere. The destabilization of SOM in the EDDS-added rhizosphere can be driven by two main mechanisms. One mechanism is the direct dissolution: EDDS solubilized Fe from iron oxides and released the Fe-protected SOM, as suggested by the high path coefficients between EDDS and Fe (0.963), and between EDDS and soil DOM (0.991). The tannin and condensed aromatic-like compounds that were usually adsorbed on iron oxides were thus observed to increase in the DOM pool (Fig. 5b) (Han et al., 2021; Huang et al., 2019). The dissolution of soil minerals and organic matter has been previously reported in heavy metal-polluted soils washed by EDDS or EDTA (Tsang et al., 2007; Zhang et al., 2010). Another mechanism is known as the “priming effect”: the EDDS was partly degraded after application which provided a fresh source of carbon and nitrogen for soil microbes, stimulated microbial growth and activities, thereby promoting the

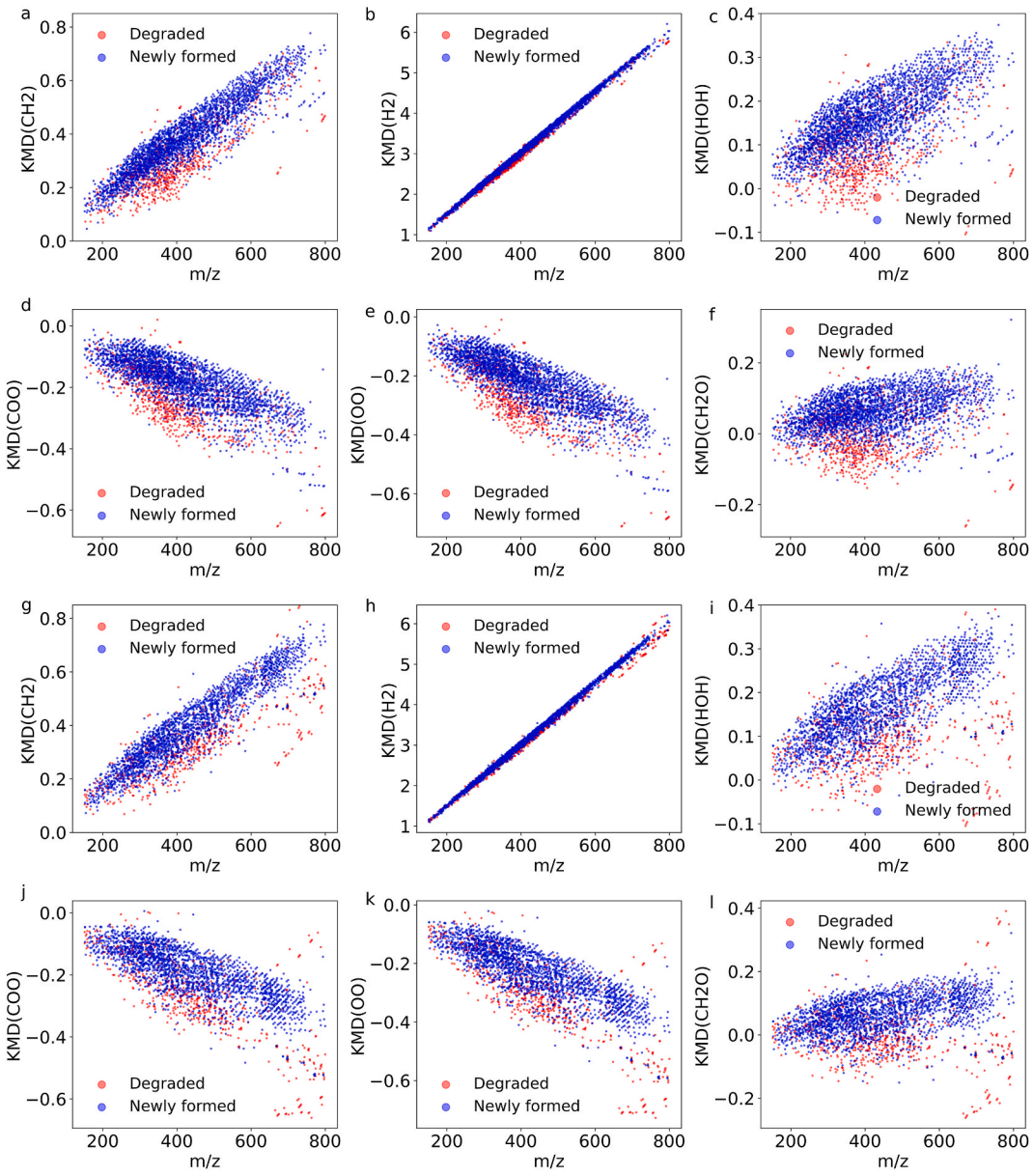

Fig. 6. Kendrick mass defect (KMD) plots for degraded and newly formed DOM molecules in control and EDDS-added soils from rhizosphere (a–f) and non-rhizosphere (g–l) based on functional groups of -CH_2, -H_2, -HOH, -COO, -OO and -CH_2O.

co-metabolism of BDOM species, as supported by the degradation of EDDS and the strong positive correlation between EDDS and microbial activities (0.735) (Fig. 7a). EDDS promoted the transformation and mineralization of BDOM species, involving lipid and protein/amino sugar-like compounds, through chain scission, dehydration, carboxylation, and hydroxylation (Fig. 6). The similar "priming effect" was often reported by low-molecular-weight acids (LMWOAs), such as oxalic acid (Ding et al., 2021).

3.7. Implication for phytoremediation

Phytoremediation has been considered as a carbon-negative technology and recommended for remediating polluted soils and mitigating climate warming, because plants can remove heavy metals from soils as well as CO_2 from the air (Khalid et al., 2016; Simmer and Schnoor, 2022). However, our study revealed that the application of the chelating agent EDDS increased the uptake of heavy metals by plants, but at the expense of destabilizing SOM, which would affect the carbon efflux during phytoremediation. On the one hand, the EDDS-induced soil dissolution can cause the carbon loss from surface soil, especially during periods of heavy rainfall. The leached soil DOM can be transported through surface runoff and potentially mineralized or released as gas in river or groundwater ecosystems (Chen et al., 2022). Additionally, EDDS-assisted phytoremediation is a long-term engineering project that can span several years or even decades. EDDS is typically added multiple times to soils to enhance the efficiency of phytoremediation for heavy metals. The repeated application of EDDS could exaggerate the problem of SOM leaching. On the other hand, EDDS can also activate soil microbes and accelerate the mineralization of BDOM to CO_2 through "priming effect". So, the application of EDDS can partly increase the emission of CO_2 from soils and decrease the capacity of carbon sequestration by plants. More studies are needed to quantitatively assess the impacts of EDDS on the rate of soil respiration and SOC mineralization at lab or field scales. Other chelating agents, such as citric acid, oxalic acid, and nitrilotriacetic acid (NTA), that are frequently employed to enhance the efficiency of phytoremediation for heavy metals (Li et al., 2020),

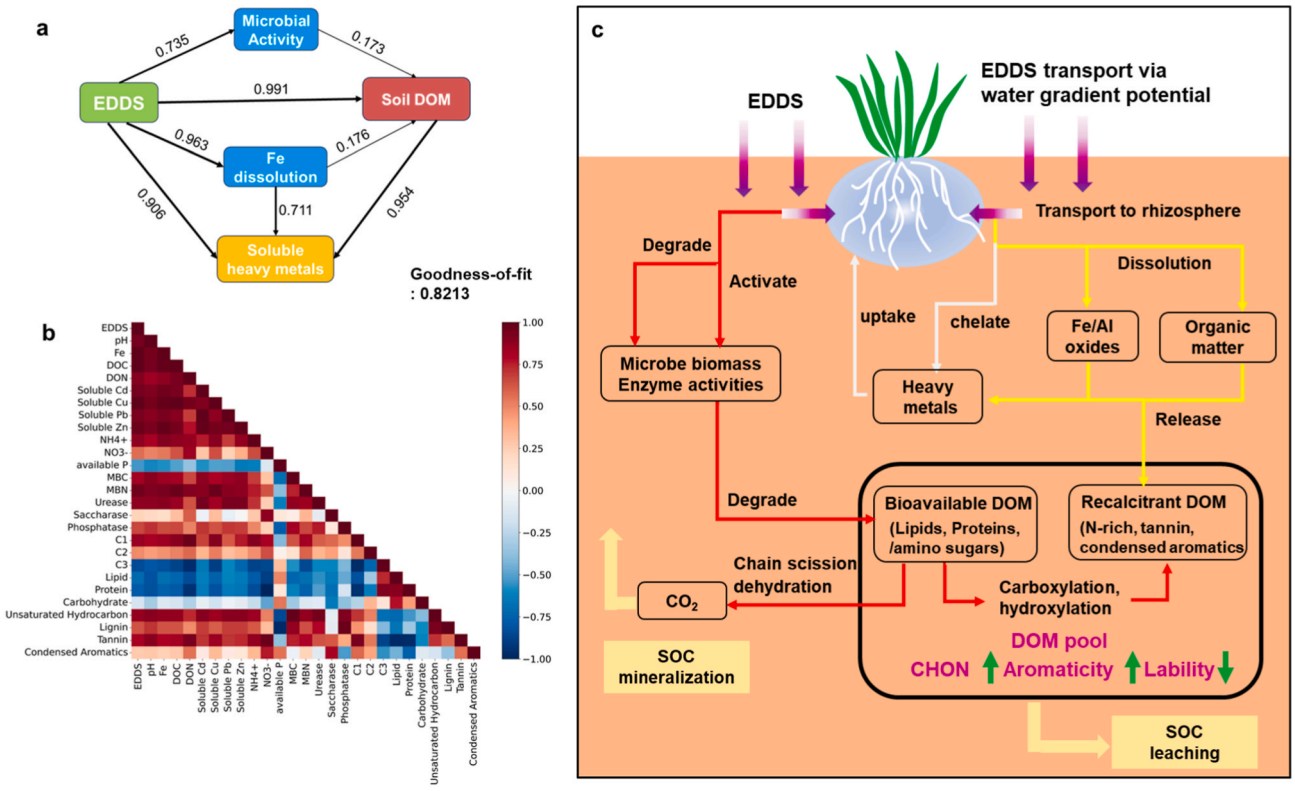

Fig. 7. Partial least squares path modeling (PLS-PM) (a) and correlation (b) of EDDS, soil physiochemical properties, microbial indexes, and DOM characteristics; Conceptual model showing the mechanism of rhizosphere soil dissolution and molecular transformation induced by EDDS (c). In panel a, solid and dotted arrows represent positive and negative effects, respectively. The values and width of the arrow in subgraph (a) refer to the strength of the standardized path coefficient.

may have similar destabilizing effects on SOM as EDDS. Therefore, the stability and turnover of SOC during phytoremediation deserve more attention in the future, particularly when chelating agents were used to enhance phytoremediation efficiency. In addition, other chelating agents can be considered as alternatives to EDDS such as humic acid to accelerate phytoremeidation efficiency without producing "priming effect" (Halim et al., 2003), in order to achieve a win-win strategy for both soil remediation and carbon sequestration.

4. Conclusion

This study was undertaken to examine the stability of SOM in the ryegrass rhizosphere following the application of EDDS, focusing on changes in both the quantity and composition of soil DOM. The findings revealed a dual impact of EDDS on SOM dynamics. Firstly, EDDS facilitated the extraction of Fe and Al, releasing associated organic compounds, such as lipids (characterized by a high C/O ratio), tannins, and condensed aromatics, into the DOM pool. Simultaneously, EDDS stimulated microbial biomass and enzyme activities by supplying fresh carbon (C) and nitrogen (N), thereby promoting the degradation of native biodegradable DOM (BDOM), including lipids, proteins/amino sugars, and lignin-like compounds. Furthermore, the transportation of EDDS from the non-rhizosphere to the rhizosphere intensified the dissolution of SOM and the degradation of BDOM in the rhizosphere. This molecular-level analysis of soil DOM significantly expands our understanding of soil organic carbon stabilization during EDDS-assisted phytoremediation. The study underscores the efficacy of molecular investigations into soil DOM as a valuable approach for observing soil carbon cycling. Notably, the research sheds light on the potential risks of soil organic carbon loss and emission following EDDS application. Further studies are warranted to explore the effects of different chelating agents on alterations in soil organic carbon during phytoremediation. Such investigations are crucial for developing strategies to control carbon emissions in soil remediation practices. In summary, the molecular insights gained from this study provide a foundation for advancing our comprehension of the intricate processes involved in carbon dynamics within phytoremediation.

CRediT authorship contribution statement

Yan-ping Zhao: Writing – original draft, Visualization, Investigation, Formal analysis, Conceptualization. **Peng-ran Guo:** Writing – review & editing, Supervision, Funding acquisition. **Zhi-liang Chen:** Project administration, Funding acquisition, Conceptualization. **Jin-li Cui:** Writing – review & editing, Resources, Methodology. **Jian-xu Wang:** Writing – review & editing, Resources. **Chao Chen:** Methodology, Data curation. **Hang Wei:** Visualization, Resources. **Cheng Wang:** Validation, Resources.

Declaration of competing interest

The authors declare that they have no known competing financial interests or personal relationships that could have appeared to influence the work reported in this paper.

Data availability

Data will be made available on request.

Acknowledgements

This work was financially supported by the National Natural Science Foundation of China (No.42307044, 42277201, 42377262, 42307337), the GDAS' Project of Science and Technology Development (No.2023GDASZH-2023010103), the Joint Funds of the National Natural Science Foundation of China (No. U22A20606), and the Foshan

Social Science and Technology Research Special Project (No. 2220001018511). Special thanks go to Dr. Jin-wei Xu for language polishing.

Appendix A. Supplementary data

Supplementary data to this article can be found online at https://doi.org/10.1016/j.envres.2024.120085.

References

Antoniadis, V., Shaheen, S.M., Levizou, E., Shahid, M., 2019. A critical prospective analysis of the potential toxicity of trace element regulation limits in soils worldwide: are they protective concerning health risk assessment? - a review. Environ. Int. 127, 819–847. https://doi.org/10.1016/j.envint.2019.03.039.

Attinti, R., Barrett, K.R., Datta, R., Sarkar, D., 2017. Ethylenediaminedisuccinic acid (EDDS) enhances phytoextraction of lead by vetiver grass from contaminated residential soils in a panel study in the field. Environ. Pollut. 225, 524–533. https://doi.org/10.1016/j.envpol.2017.01.088.

Begum, Z.A., Rahman, I.M.M., Ishii, K., Tsukada, H., Hasegawa, H., 2020. Dynamics of Strontium and geochemically correlated elements in soil during washing remediation with eco-complaint chelators. J. Environ. Manage. 259, 110018. https://doi.org/10.1016/j.jenvman.2019.110018.

Beillouin, D., Corbeels, M., Demenois, J., Berre, D., Boyer, A., Fallot, A., Feder, F., Cardinael, R., 2023. A global meta-analysis of soil organic carbon in the Anthropocene. Nat. Commun. 14, 3700. https://doi.org/10.1038/s41467-023-39338-z.

Beiyuan, J., Tsang, D.C.W., Valix, M., Zhang, W., Yang, X., Ok, Y.S., Li, X.D., 2017. Selective dissolution followed by EDDS washing of an e-waste contaminated soil: extraction efficiency, fate of residual metals, and impact on soil environment. Chemosphere 166, 489–496. https://doi.org/10.1016/j.chemosphere.2016.09.110.

Cater, M.R., Gregorich, E.G., 2006. Soil Sampling and Methods of Analysis. CRC press.

Chen, H.B., Gao, Y.R., Dong, H.Y., Sarkar, B., Song, H., Li, J.H., Bolan, N., Quin, B.F., Yang, X., Li, F.B., Wu, F.C., Meng, J., Wang, H.L., Chen, W.F., 2023. Chitin and crawfish shell biochar composite decreased heavy metal bioavailability and shifted rhizosphere bacterial community in an arsenic/lead co-contaminated soil. Environ. Int. 176, 107989. https://doi.org/10.1016/j.envint.2023.107989.

Chen, L. tao, Liu, T., Ma, C.A., 2010. Metal complexation and biodegradation of EDTA and S,S-EDDS: a density functional theory study. J. Phys. Chem. A 114, 443–454. https://doi.org/10.1021/jp904296m.

Chen, L.Y., Liu, L., Qin, S.Q., Yang, G.B., Fang, K., Zhu, B., Chen, P.D., Xu, Y.P., Yang, Y. H., Kuzyakov, Y., 2019. Regulation of priming effect by soil organic matter stability over a broad geographic scale. Nat. Commun. 10, 5112. https://doi.org/10.1038/s41467-019-13119-z.

Chen, X., Qin, X.B., Li, Y., Wan, Y.F., Liao, Y.L., Lu, Y.H., Wang, B., Chen, H.R., Wang, K. Y., 2022. Residential and agricultural soils dominate soil organic matter loss in a typical agricultural watershed of subtropical China. Agric. Ecosyst. Environ. 338, 108100. https://doi.org/10.1016/j.agee.2022.108100.

Dick, R.P., 2011. Methods of Soil Enzymology. Soil Science Society of America, Madison.

Ding, Y., Ye, Q.T., Liu, M.Q., Shi, Z.Q., Liang, Y.Z., 2021. Reductive release of Fe mineral-associated organic matter accelerated by oxalic acid. Sci. Total Environ. 763, 142937. https://doi.org/10.1016/j.scitotenv.2020.142937.

Dittmar, T., Koch, B., Hertkorn, N., Kattner, G., 2008. A simple and efficient method for the solid-phase extraction of dissolved organic matter (SPE-DOM) from seawater. Limnol. Oceanogr. 6, 230–235. https://doi.org/10.4319/lom.2008.6.230.

Eivazi, F., Tabatabai, M.A., 1977. Phosphatase in soils. Soil Biol. Biochem. 9, 167–172.

El-naggar, A., Lee, M., Hur, J., Han, Y., Deshani, A., Shaheen, S.M., Ryu, C., Rinklebe, J., Tsang, D.C.W., Sik, Y., 2020. Biochar-induced metal immobilization and soil biogeochemical process : an integrated mechanistic approach. Sci. Total Environ. 698, 134112. https://doi.org/10.1016/j.scitotenv.2019.134112.

Fang, L.C., Wang, M.K., Cai, L., Cang, L., 2017. Deciphering biodegradable chelant-enhanced phytoremediation through microbes and nitrogen transformation in contaminated soils. Environ. Sci. Pollut. Res. 24, 14627–14636. https://doi.org/10.1007/s11356-017-9029-y.

Fu, Q.L., Fujii, M., Riedel, T., 2020. Development and comparison of formula assignment algorithms for ultrahigh-resolution mass spectra of natural organic matter. Anal. Chim. Acta 1125, 247–257. https://doi.org/10.1016/j.aca.2020.05.048.

Gan, S.C., Guo, P.R., Wu, Y., Zhao, Y.P., 2021. A novel method for unraveling the black box of dissolved organic matter in soils by FT-ICR-MS coupled with induction-based nanospray ionization. Environ. Sci. Technol. Lett. 8, 356–361. https://doi.org/10.1021/acs.estlett.1c00095.

Garbisu, C., Alkorta, I., 2001. Phytoextraction: a cost-effective plant-based technology for the removal of metals from the environment. Bioresour. Technol. 77, 229–236. https://doi.org/10.1016/S0960-8524(00)00108-5.

Gong, C., Jiao, R.Y., Yan, W.J., Yu, Q.B., Li, Q.Q., Zhang, P.P., Li, Y., Wang, D.S., 2022. Enhanced chemodiversity, distinctive molecular signature and diurnal dynamics of dissolved organic matter in streams of two headwater catchments. Southeastern China. Water Res 211, 118052. https://doi.org/10.1016/j.watres.2022.118052.

Gu, Z.P., Bao, M., He, C., Chen, W.M., 2023. Transformation of dissolved organic matter in landfill leachate during a membrane bioreactor treatment. Sci. Total Environ. 856, 159066. https://doi.org/10.1016/j.scitotenv.2022.159066.

Guan, S.Y., 1986. Soil Enzymes and its Research Approaches. China Agriculture Press, Beijing (in Chinese).

Halim, M., Conte, P., Piccolo, A., 2003. Potential availability of heavy metals to phytoextraction from contaminated soils induced by exogenous humic substances. Chemosphere 52 (1), 265–275. https://doi.org/10.1016/S0045-6535(03)00185-1.

Han, H., Wu, X.J., Yao, L.G., Chen, Z.J., 2020. Heavy metal-immobilizing bacteria combined with calcium polypeptides reduced the uptake of Cd in wheat and shifted the rhizosphere bacterial communities. Environ. Pollut. 267, 115432. https://doi.org/10.1016/j.envpol.2020.115432.

Han, H.X., Feng, Y.J., Chen, J., Xie, Q.R., Chen, S., Sheng, M., Zhong, S.J., Wei, W., Su, S. H., Fu, P.Q., 2022. Acidification impacts on the molecular composition of dissolved organic matter revealed by FT-ICR MS. Sci. Total Environ. 805, 150284. https://doi.org/10.1016/j.scitotenv.2021.150284.

Han, L.F., Yang, Y., Sun, K., Zhang, B., Chen, Y.L., Fang, L.P., Xing, B.S., 2021. Different mechanisms driving the preferential adsorption of dissolved organic matter by goethite and montmorillonite. Chem. Geol. 585, 120560. https://doi.org/10.1016/j.chemgeo.2021.120560.

Harmon, S.M., 2022. Biodegradable chelate-assisted phytoextraction of metals from soils and sediments. Curr. Opin. Green Sustain. Chem. 37, 100677. https://doi.org/10.1016/j.cogsc.2022.100677.

Huang, M., Zhou, M., Li, Z.W., Ding, X., Wen, J.J., Jin, C.S., 2022. How do drying-wetting cycles influence availability of heavy metals in sediment ? A perspective from DOM molecular composition. Water Res. 220, 118671. https://doi.org/10.1016/j.watres.2022.118671.

Huang, Z.Q., Lv, J.T., Cao, D., Zhang, S.Z., 2019. Iron plays an important role in molecular fractionation of dissolved organic matter at soil-water interface. Sci. Total Environ. 670, 300–307. https://doi.org/10.1016/j.scitotenv.2019.03.214.

Ishii, S.K.L., Boyer, T.H., 2012. Behavior of reoccurring PARAFAC components in fluorescent dissolved organic matter in natural and engineered systems: a critical review. Environ. Sci. Technol. 46 (4), 2006–2017. https://doi.org/10.1021/es2043504.

Ju, W.L., Liu, L., Jin, X.L., Duan, C.J., Cui, Y.X., Wang, J., Ma, D.K., Zhao, W., Wang, Y. Q., Fang, L.C., 2020. Co-inoculation effect of plant-growth-promoting rhizobacteria and rhizobium on EDDS assisted phytoremediation of Cu contaminated soils. Chemosphere 254, 126724. https://doi.org/10.1016/j.chemosphere.2020.126724.

Katata, L., Nagaraju, V., Crouch, A.M., 2006. Determination of ethylenediaminetetraacetic acid, ethylenediaminedisuccinic acid and iminodisuccinic acid in cosmetic products by capillary electrophoresis and high performance liquid chromatography. Anal. Chim. Acta 579, 177–184. https://doi.org/10.1016/j.aca.2006.07.024.

Kaurin, A., Gluhar, S., Tilikj, N., Lestan, D., 2020. Soil washing with biodegradable chelating agents and EDTA: effect on soil properties and plant growth. Chemosphere 260, 127673. https://doi.org/10.1016/j.chemosphere.2020.127673.

Khalid, S., Shahid, M., Niazi, N.K., Murtaza, B., Bibi, I., Dumat, C., Khalid, S., Shahid, M., Niazi, N.K., Murtaza, B., Bibi, I., 2016. A comparison of technologies for remediation of heavy metal contaminated soils to cite this version : HAL Id : hal-01577861. J. Geochemical Explor. 182, 247–268. https://doi.org/10.1016/j.gexplo.2016.11.021.

Li, C., Xiao, C.W., Li, M.X., Xu, L., He, N.P., 2023. The quality and quantity of SOM determines the mineralization of recently added labile C and priming of native SOM in grazed grasslands. Geoderma 432, 116385. https://doi.org/10.1016/j.geoderma.2023.116385.

Komárek, M., Vaněk, A., Száková, J., Balík, J., Chrastný, V., 2009. Interactions of EDDS with Fe- and Al-(hydr)oxides. Chemosphere 77 (1), 87–93. https://doi.org/10.1016/j.chemosphere.2009.05.021.

Li, H., Bo, T., Winnick, M., Tfaily, M.M., Cardon, Z.G., Keiluweit, M., 2021. Simple plant and microbial exudates destabilize mineral-associated organic matter via multiple pathways. Environ. Sci. Technol. 55, 3389–3398. https://doi.org/10.1021/acs.est.0c04592.

Li, J.Q., He, E., Romero-freire, A., Cao, X. De, Zhao, L., Qiu, H., 2020. Coherent toxicity prediction framework for deciphering the joint effects of rare earth metals (La and Ce) under varied levels of calcium and NTA. Chemosphere 254, 126905. https://doi.org/10.1016/j.chemosphere.2020.126905.

Luo, C.L., Shen, Z.G., Li, X.D., Baker, A.J.M., 2006. Enhanced phytoextraction of Pb and other metals from artificially contaminated soils through the combined application of EDTA and EDDS. Chemosphere 63, 1773–1784. https://doi.org/10.1016/j.chemosphere.2005.09.050.

Luo, C.L., Wang, S.R., Wang, Y., Yang, R.X., Zhang, G., Shen, Z.G., 2015. Effects of EDDS and plant-growth-promoting bacteria on plant uptake of trace metals and PCBs from e-waste-contaminated soil. J. Hazard Mater. 286, 379–385. https://doi.org/10.1016/j.jhazmat.2015.01.010.

Lv, J.T., Zhang, S.Z., Wang, S.S., Luo, L., Cao, D., Christie, P., 2016. Molecular-Scale investigation with ESI-FT-ICR-MS on fractionation of dissolved organic matter induced by adsorption on iron oxyhydroxides. Environ. Sci. Technol. 50, 2328–2336. https://doi.org/10.1021/acs.est.5b04996.

Margesin, R., Schinner, F., 2005. Manual for Soil Analysis - Monitoring and Assessing Soil Bioremediation. Springer Science & Business Media, Berlin, Heidelberg.

Mostofa, K.M.G., Jie, Y., Sakugawa, H., Liu, C.Q., 2019. Equal treatment of different EEM data on PARAFAC modeling produces artifact fluorescent components that have misleading biogeochemical consequences. Environ. Sci. Technol. 53, 561–563. https://doi.org/10.1021/acs.est.8b06647.

Ohno, T., 2002. Fluorescence inner-filtering correction for determining the humification index of dissolved organic matter. Environ. Sci. Technol. 36, 742–746. https://doi.org/10.1021/es0155276.

Perminova, I.V., Dubinenkov, I.V., Kononikhin, A.S., Konstantinov, A.I., Zherebker, A.Y., Andzhushev, M.A., Lebedev, V.A., Bulygina, E., Holmes, R.M., Kostyukevich, Y.I., Popov, I.A., Nikolaev, E.N., 2014. Molecular mapping of sorbent selectivities with respect to isolation of Arctic dissolved organic matter as measured by Fourier

transform mass spectrometry. Environ. Sci. Technol. 48 (13), 7461–7468. https://doi.org/10.1021/es5015423.
Piccolo, A., Drosos, M., 2024. The supramolecular structure of the soil humeome and the significance of humification. Adv. Agron. 188, 405–455. https://doi.org/10.1016/bs.agron.2024.06.006.
Qi, Y.L., Xie, Q.R., Wang, J.J., He, D., Bao, H.Y., Fu, Q.L., Su, S.H., Sheng, M., Li, S.L., Volmer, D.A., Wu, F.C., Jiang, G. Bin, Liu, C.Q., Fu, P., 2022. Deciphering dissolved organic matter by Fourier transform ion cyclotron resonance mass spectrometry (FT-ICR MS): from bulk to fractions and individuals. Carbon Res 1–22. https://doi.org/10.1007/s44246-022-00002-8.
Santana-casiano, J.M., Gonz, D., Devresse, Q., Hepach, H., Santana-gonz, C., Quack, B., Engel, A., Gonz, M., 2022. Exploring the effects of organic matter characteristics on Fe (II) oxidation kinetics in coastal seawater. Environ. Sci. Technol. 56 (4), 2718–2728. https://doi.org/10.1021/acs.est.1c04512.
Sheng, M., Chen, S., Liu, C.Q., Fu, Q.L., Zhang, D.H., Hu, W., Deng, J.J., Wu, L. Bin, Li, P., Yan, Z.F., Zhu, Y.G., Fu, P.Q., 2023. Spatial and molecular variations in forest topsoil dissolved organic matter as revealed by FT-ICR mass spectrometry. Sci. Total Environ. 895, 165099. https://doi.org/10.1016/j.scitotenv.2023.165099.
Simmer, R.A., Schnoor, J.L., 2022. Phytoremediation, bioaugmentation, and the plant microbiome. Environ. Sci. Technol. 56, 16602–16610. https://doi.org/10.1021/acs.est.2c05970.
Stedmon, C.A., Bro, R., 2008. Characterizing dissolved organic matter fluorescence with parallel factor analysis: a tutorial. Limnol. Oceanogr. 6, 572–579. https://doi.org/10.4319/lom.2008.6.572.
Tang, S.Q., Liang, J.M., Xu, X.M., Jin, Y.S., Xuan, W.W., Li, O.Y., Fang, L., Li, Z.S., 2023. Targeting phosphorus transformation to hydroxyapatite through sewage sludge pyrolysis boosted by quicklime toward phosphorus fertilizer alternative with toxic metals compromised. Renew. Sustain. Energy Rev. 183, 113474. https://doi.org/10.1016/j.rser.2023.113474.
Trainer, E.L., Ginder-Vogel, M., Remucal, C.K., 2021. Selective reactivity and oxidation of dissolved organic matter by manganese oxides. Environ. Sci. Technol. 55 (17), 12084–12094. https://doi.org/10.1021/acs.est.1c03972.
Tsang, D.C.W., Yip, T.C.M., Lo, I.M.C., 2009. Kinetic interactions of EDDS with soils. 2. metal−EDDS complexes in uncontaminated and metal-contaminated soils. Environ. Sci. Technol. 43, 837–842. https://doi.org/10.1021/es8020292.
Tsang, D.C.W., Zhang, W., Lo, I.M.C., 2007. Copper extraction effectiveness and soil dissolution issues of EDTA-flushing of artificially contaminated soils. Chemosphere 68, 234–243. https://doi.org/10.1016/j.chemosphere.2007.01.022.
Tu, C., Wei, J., Guan, F., Liu, Y., Sun, Y.H., Luo, Y.M., 2020. Biochar and bacteria inoculated biochar enhanced Cd and Cu immobilization and enzymatic activity in a polluted soil. Environ. Int. 137, 105576. https://doi.org/10.1016/j.envint.2020.105576.
Vance, E.D., Brookes, P.C., Jenkinson, D.S., 1987. An extraction method for measuring soil microbial biomass C. Soil Biol. Biochem. 19, 703–707. https://doi.org/10.1016/0038-0717(87)90052-6.
Wang, C., Wang, J.H., Zhong, C., Zhao, Y.P., 2023. Divergent temporal changes of heavy metals in the soil induced by natural versus anthropogenic forces: a case study in the Yangtze River delta area, China. Sci. Total Environ. 894, 165054. https://doi.org/10.1016/j.scitotenv.2023.165054.
Wang, G.Y., Zhang, S.R., Zhong, Q.M., Peijnenburg, W.J.G.M., Vijver, M.G., 2018. Feasibility of Chinese cabbage (Brassica bara) and lettuce (Lactuca sativa) cultivation in heavily metals−contaminated soil after washing with biodegradable chelators. J. Clean. Prod. 197, 479–490. https://doi.org/10.1016/j.jclepro.2018.06.225.
Wang, J.J., Liu, Y.N., Bowden, R.D., Lajtha, K., Simpson, A.J., Huang, W.L., Simpson, M. J., 2020. Long-term nitrogen addition alters the composition of soil- derived dissolved organic matter. ACS Earth Sp. Chem. 4, 189–201. https://doi.org/10.1021/acsearthspacechem.9b00262.
Wang, X.L., Fernandes, M., Souza, D., Mench, M.J., Li, H.C., Sik, Y., Tack, F.M.G., Meers, E., 2022a. Cu phytoextraction and biomass utilization as essential trace element feed supplements for livestock. Environ. Pollut. 294, 118627. https://doi.org/10.1016/j.envpol.2021.118627.
Wang, Z., Han, R.X., Muhammad, A., Guan, D.X., Zama, E., 2022b. Correlative distribution of DOM and heavy metals in the soils of the Zhangxi watershed in Ningbo city , East of China. Environ. Pollut. 299, 118811. https://doi.org/10.1016/j.envpol.2022.118811.
Wu, L. Bin, Sheng, M., Liu, X.D., Zheng, Z.Q., Emslie, S.D., Yang, N., Wang, X.Y., Nie, Y. G., Jin, J., Xie, Q.R., Chen, S., Zhang, D.H., 2023. Molecular transformation of organic nitrogen in Antarctic penguin guano-affected soil. Environ. Int. 172, 107796. https://doi.org/10.1016/j.envint.2023.107796.
Xu, H.W., You, C.M., Tan, B., Xu, L., Liu, Y., Wang, M.G., Xu, Z.F., Sardans, J., Peñuelas, J., 2023. Effects of livestock grazing on the relationships between soil microbial community and soil carbon in grassland ecosystems. Sci. Total Environ. 881, 163416. https://doi.org/10.1016/j.scitotenv.2023.163416.
Yang, L., Wang, G.P., Cheng, Z.N., Liu, Y., Shen, Z.G., Luo, C.L., 2013. Influence of the application of chelant EDDS on soil enzymatic activity and microbial community structure. J. Hazard Mater. 262, 561–570. https://doi.org/10.1016/j.jhazmat.2013.09.009.
Yang, R.X., Luo, C.L., Zhang, G., Li, X.D., Shen, Z.G., 2012. Extraction of heavy metals from e-waste contaminated soils using EDDS. J. Environ. Sci. 24, 1985–1994. https://doi.org/10.1016/S1001-0742(11)61036-X.
Yao, A.J., Ju, L., Ling, X.D., Liu, C., Wei, X.E., Qiu, H., Tang, Y.T., Louis, J., Qiu, R.L., Li, C., Wang, S.Z., 2019. Simultaneous attenuation of phytoaccumulation of Cd and as in soil treated with inorganic and organic amendments. Environ. Pollut. 250, 464–474. https://doi.org/10.1016/j.envpol.2019.04.073.
Yi, H.L., Cui, J.L., Sun, J.T., Zhou, X.Y., Ye, T.C., Gan, S.C., Chen, J.C., Yang, Y.Z., Liang, W.X., Guo, P.R., Abdelhaleem, A., 2023. Key drivers regulating arsenic enrichment in shallow groundwater of the Pearl River Delta: comprehensive analyses of iron, competitive anions, and dissolved organic matter. Appl. Geochemistry 151, 105602. https://doi.org/10.1016/j.apgeochem.2023.105602.
Yip, T.C.M., Tsang, D.C.W., Ng, K.T.W., Lo, I.M.C., 2009. Kinetic interactions of EDDS with soils. 1. metal resorption and competition under EDDS deficiency. Environ. Sci. Technol. 43, 831–836. https://doi.org/10.1021/es802030k.
Zhang, W.H., Huang, H., Tan, F.F., Wang, H., Qiu, R.L., 2010. Influence of EDTA washing on the species and mobility of heavy metals residual in soils. J. Hazard Mater. 173, 369–376. https://doi.org/10.1016/j.jhazmat.2009.08.087.
Zhao, F.J., Ma, Y.B., Zhu, Y.G., Tang, Z., McGrath, S.P., 2015. Soil contamination in China: current status and mitigation strategies. Environ. Sci. Technol. 49, 750–759. https://doi.org/10.1021/es5047099.
Zhao, Y.P., Cui, J.L., Chan, T.S., Chen, Y.H., Li, X.D., 2020. Mechanistic insight into the interactions of EDDS with copper in the rhizosphere of polluted soils. Environ. Pollut. 267, 115453. https://doi.org/10.1016/j.envpol.2020.115453.